J Appl Electrochem (2010) 40:1593–1603
DOI 10.1007/s10800-010-0144-4

ORIGINAL PAPER

# Separation and direct detection of heavy lanthanides using new ion-exchange chromatography: fast Fourier transform continuous cyclic voltammetry system

**Mohammad Reza Pourjavid · Parviz Norouzi · Hamid Rashedi · Mohammad Reza Ganjali**

Received: 10 July 2009 / Accepted: 18 April 2010 / Published online: 29 April 2010


**Abstract** In this study, possibilities of heavy lanthanides ($Ho^{3+}$, $Er^{3+}$, $Tm^{3+}$, $Yb^{3+}$, and $Lu^{3+}$) separation on Nucleosil 100-5-SA, an ion-exchange column, was investigated. Separation of lanthanides was carried out using an isocratic program of α-hydroxyisobutyric acid (HIBA) eluent. Fast Fourier transform continuous cyclic voltammetry (FFT-CCV) at a gold microelectrode was used as the detection method. Simplicity, high precision and accuracy, time efficiency, and being economic are advantages of the developed technique in comparison with the previous reported ones. In addition, removal of oxygen from the test solution is not required, the detection limit is suitable and the technique is fast enough for determination of compounds in a wide variety of chromatographic methods. The waveform potential was continuously applied on an Au disk microelectrode (12.5 μm in radius). The influence of HIBA concentration as well as pH of eluent was optimized. The best performance of the method was obtained at pH of 4.0, scan rate of 30 V $s^{-1}$, accumulation potential of −300 mV, and accumulation time of 0.3 s. The proposed method displays a linear dynamic range of 140 and 18,000 μg $L^{-1}$ and a detection limit of 50 μg $L^{-1}$. Precision, inter-day precision, and accuracy of the assay were reported too. A comparative evaluation of heavy lanthanides distributed in a sophisticated monazite and xenotime minerals solutions was carried out using both FFT-CCV, and inductively coupled plasma-atomic emission spectrometry (ICP-AES).

**Keywords** Heavy lanthanides · α-Hydroxyisobutyric acid · Flow injection · Fast Fourier transform continuous cyclic voltammetry

M. R. Pourjavid · P. Norouzi · M. R. Ganjali (✉)
Center of Excellence in Electrochemistry, Faculty of Chemistry, University of Tehran, Tehran, Iran
e-mail: ganjali@khayam.ut.ac.ir

H. Rashedi
Department of Biochemistry Engineering, Faculty of Engineering, University of Tehran, Tehran, Iran

## 1 Introduction

For many years, chemists were involved in separation of lanthanides. Separation of these elements causes considerable challenges due to the marked similarity in their chemical and physical properties (especially charge and ionic radii), and also due to their flexibility in the formation of coordination compounds. Also, they always find with each other in the nature at trace concentration levels. It makes their separation as a group or individuals extremely difficult. There are many articles about the methods of lanthanide separation, but among them high performance liquid chromatography (HPLC), ion chromatography (IC), and capillary electrophoresis (CE) have the most utilization [1–11]. Researches explain the use of high performance liquid chromatography, cation- and/or anion-exchange chromatography, and capillary electrophoresis for separation of lanthanide ions with UV–Vis spectrometry, refractive index (RI), spectrofluorimetry, ICP-AES and diode array detectors. Many of these attempts have used the differences between stability constants of lanthanide ions with a particular complexing agent to achieve a satisfactory separation. Molecules with a flexible structure can reorient its coordination site around the lanthanide(III) ions, while the cation size changes, and, therefore, have similar stability constants for these trivalent metal ions. A more rigid coordination structure could decrease the stability constant

of the ligand, but increase the size selectivity of the ligand to lanthanide(III) ion due to the varied coordination distances and the different radii of the ions. Such compounds could provide improved materials for the separation of these ions [12].

In general, ion chromatography is an attractive procedure for analysis of lanthanides. In this method, low-capacity cation-exchange resins are typically used as stationary phases, and mobile phases are aqueous solutions of complexing agents. Many eluents, such as α-hydroxyisobutyric acid (α-HIBA) [13–15], mandelic acid [16], oxalic acid [17], glycolic acid [18], lactic acid [19], etc., have been used for lanthanide separation. Fernández and Alonso [20] recently used ethylenediaminetetraacetic acid (EDTA) as a mobile phase in the separation of lanthanides. A mixed gradient of two eluents has also been used in some researches [13, 21]. The most popular eluting agent in these works is HIBA due to a good degree of separation among adjacent lanthanides. HIBA forms complexes with lanthanide ions, and decreases the affinity of the lanthanide to cation-exchange resin. In this case, two equilibriums should be considered: the equilibrium between the eluent and the resin, and the equilibrium between the lanthanide and the lanthanide–HIBA complex. Each lanthanide will spend more or less time in the eluent due to the stability constant of its complex with HIBA. Therefore, lanthanides such as Lu (which forms the most stable complex with HIBA), will spend relatively more time in the eluent and elute first. Conversely, lanthanides that form a weaker complex with HIBA (such as Ho) spend relatively less time in the eluent. These cations spend more time in the resin and elute later. Also, HIBA was found to be better eluent for heavy lanthanides and its LOD is a little bit less than medium or light lanthanides. Stronger complexing agents, such as oxalic acid, form complexes with negative charges. Under these conditions, the lanthanide series may be separated by anion-exchange chromatography. Since the strongest complexes are the most negatively charged, the elution order is reversed from that of the cation-exchange separations. Thus, HIBA was used as an eluting agent in this study.

One of the general methods for determination of separated lanthanides is the post-column derivatization method. This normally involves the use of UV–Vis detection at wavelengths ranging from 512 to 658 nm. Arsenazo-III and PAR are the most commonly used complexing reagents [7, 22]. In the past years, ICP-AES and ICP-MS interfaced with ion chromatography have been used in simultaneous and multi-element analysis of lanthanide [23, 24]. Occasionally, a large amount of reagent used as the mobile phase causes spectral interference. In addition, the high viscosity of concentrated salt solutions tends to influence the nebulization efficiency. The interferences due to polyatomic ions cause a serious problem in the case of ICP-MS [25]. Electrochemical methods can be also useful tools for lanthanide determination. Potentiometric sensors can offer an acceptable sensitivity, selectivity, inexpensive, and convenient method for rare-earth ions analysis in solution. There are many reports about ion selective electrodes (ISEs) for lanthanide ions in last decade [26–35]. In this study, fast Fourier transform continuous cyclic voltammetry (FFT-CCV) was investigated as a new method for determination of holmium, erbium, thulium, ytterbium, and lutetium. Detection of lanthanide ions with FFT-CCV is faster than other detection methods, especially UV–Vis spectrometry, because in these methods, pre- or post-column derivatization is necessary which is time consuming and expensive. Due to the movement of the analyte zone in an electrochemical flow cell, the application of such techniques requires fast accumulation of the analyte and also fast potential sweeping (which is not appropriate for large electrodes) [36]. In general, electrochemical measurements at solid electrodes are not suitable for the kinetically controlled or irreversible processes because the surfaces of the solid electrodes are easily deactivated (or poisoned) by products of the red/ox reactions of the desired species or by impurities present in the solution. Problems of such methods, however, can be overcome using ultramicroelectrodes (UMEs). Use of UMEs with voltammetric techniques offers advantages of steady-state currents, higher sensitivity due to increase of mass transport, and ability to be used in solutions with very high resistances [37]. For instance, UMEs have been applied as sensors in various techniques like flow injection analysis [38], cardiovascular monitoring, and in analysis of some organic compounds [39]. Another problem with solid electrodes comes from the changes in the characteristics of the electrode surface during the potential scan. The electrode signal will have a large background current. If the surface of the solid electrode is oxidized and reduced during voltammetric measurements (the response of the electrode will have a large background current), high levels of noise due to the structural changes of the electrode surface will occur. Currents like this can interfere with the desirable electrode processes and may adversely affect the detection limits of the method used.

The background current in voltammetric measurements can provide useful pieces of information about the adsorption processes and changes in the double layer at the electrode surface [40]. In addition, small amounts of adsorption of the species present in the solution on the electrode surface can strongly affect the cathodic and anodic currents of the red/ox reaction of the electrode. A special computer-based numerical method was also introduced for the calculation of the signal of the analyte and noise reduction. Signal calculation was based on the net

partial and total charge exchanges at the electrode surface, and was done by integrating the currents at the selected potential range at the cyclic voltammogram (CV). Depending on conditions applied, the detector (the proposed method) can be used in the determination of inorganic and organic species in various chromatographic analysis methods (e.g., HPLC and IC).

## 2 Experimental

### 2.1 Apparatus

Model IC760 (Metrohm) was used during the ion chromatographic experiments. Characterization of some useful cation exchangers is presented in Table 1 [41]. In the case of separation of heavy lanthanides, ion-exchanger DOWEX 50WX8 was used. The operation was completed under the flow rate 1.5 mL $min^{-1}$.

The equipment for flow injection analysis included a 10 roller peristaltic pump (UltrateckLabs Co., Iran) and a four-ways injection valve (Supelco Rheodyne Model 5020) with a 50 mL sample injection loop. Solutions were introduced into the sample loop by means of a plastic syringe. The electrochemical cell used in the flow injection analysis is shown in Fig. 1. The volume of the cell was 100 mL. In all experiments described in this article, the flow rate of eluent solution was 3 mL $min^{-1}$. The potentiostat applied a potential in the range of gold oxidation in acidic media and the potential waveform is shown in Fig. 2. A special computer program can monitor the cyclic voltammograms online as well as every current change or charge.

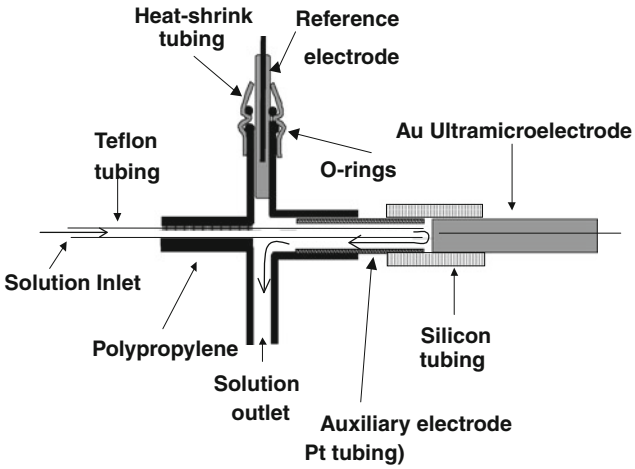


**Fig. 1** Diagram of electrochemical cell

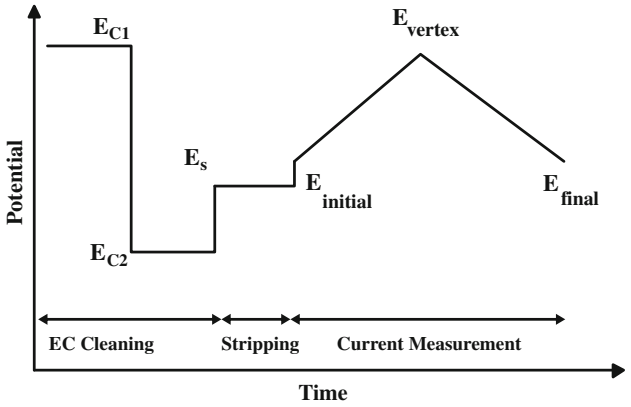


**Fig. 2** Diagram of applied potential waveform

**Table 1** Characterization of cation-exchanger

| Character | Trade name | Procedure | Active group | Matrix | Effective pH | Total exchange capacity (meq $mL^{-1}$) | Standard mesh range |
|---|---|---|---|---|---|---|---|
| SAC | Dowex 50 | 1 | Sulfonic acid | Polystyrene | 0–14 | $Na^+$ 1.9<br>$H^+$ 1.7 | 20–50 (wet) |
| SAC | Dowex MPC-1 | 4 | Sulfonic acid | Polystyrene | 0–14 | 1.6–1.8<br>$H^+$ form | 20–40 (wet) |
| SAC | Dowex 50WX8 | 1 | Sulfonic acid | Polystyrene | 0–14 | 1.7<br>$H^+$ form | 50–100 |
| SAC | Duolite C-20 | 2 | Sulfonic acid | Polystyrene | 0–14 | 2.2 | 16–50 |
| SAC | Ionac 240 | 3 | Sulfonic acid | Polystyrene | 0–14 | 1.9 | 16–50 |
| SAC | Duolite C-3 | 2 | Methylene Sulfonic | Phenolic | 0–9 | 1.1 | 16–50 |
| WAC | Dowex CCR-1 | 4 | Carboxylic | Phenolic | 0–9 | – | 20–50 (wet) |
| WAC | Duolite ES-63 | 2 | Phosphonic | Polystyrene | 4–14 | 3.3 | 16–50 |
| WAC | Duolite ES-80 | 2 | Aliphatic | Acrylic | 6–14 | 3.5 | 16–50 |

*SAC* strong acid cation, *WAC* weak acid cation, *1* Dow, *2* Diamond Shamarck, *3* Ionac, *4* Nalco

A Varian Liberty 150 AX Turbo model inductively coupled plasma-atomic emission spectroscopy (ICP-AES) was used for the determination of the lanthanide ions concentration.

### 2.2 Reagents

For the experimental, the oxide of lanthanides, hydrochloric acid, and HIBA were of high purity available from Merck Chemicals and were used without further purification. HIBA 0.2 mol $L^{-1}$ was buffered at pH 4.0 with sodium hydroxide. The reagents for preparation of the eluent solution for flow injection analysis (0.05 mol $L^{-1}$ $H_3PO_4$), and 1 mol $L^{-1}$ NaOH (for the pH eluent adjustment), were obtained (from Merck). All solutions were prepared in doubly distilled deionized water, filled with the background electrolyte solution and were used without removal of the dissolved oxygen.

### 2.3 Background electrolyte (BGE) and standard solutions

The running buffer or BGE was made by addition of 8.7 mL phosphoric acid (85% w/v) in a 1,000 mL volumetric flask, and diluted to a constant volume with distilled water. The pH was adjusted to 4.0 with sodium hydroxide and all solutions were freshly prepared and filtered using a Millipore filter (0.45 μm) daily.

A lanthanide standard stock solution was prepared by dissolving the pure oxide of lanthanides in 0.36 M hydrochloric acid. These solutions were diluted with doubly distilled deionized water to about 10 mg $L^{-1}$ of metal in standard solutions. Aliquots of standard stock solution of lanthanides were dispensed into 10 mL volumetric flasks and made up to volume with the running buffer to give a final concentration range of 10–18,000 μg $L^{-1}$.

### 2.4 Electrode preparation

Gold UMEs (12.5 mm in diameter) were prepared by sealing metal micro-wires (Good fellow Metals Ltd., Huntingdon, UK) into a soft glass capillary. The capillary was cut perpendicular to its length to expose the wire. Electrical contacts were made using silver epoxy (Johnson Matthey Ltd., London, UK). Before each experiment, the electrode surface was polished for 1 min using an extra fine carborundum paper, and then for 10 min with 0.3 mm alumina. Prior to being placed in the cell, the electrode was washed with distilled water. During all measurements, an Ag(s)|AgCl(s)|KCl (aq, 1 mol $L^{-1}$) reference electrode was used. The auxiliary electrode was made of Pt wire, 1 cm in length and 0.5 mm in diameter.

## 3 Results and discussion

### 3.1 Data acquisition and processing

For the data acquisition, the setup of a PC PIV Pentium 900 MHz microcomputer equipped with a data acquisition board (PCL-818HG, Advantech. Co.), and a custom made potentiostat were used. All data acquisition and data processing programs were developed in Delphi 6® program environment. In Fig. 2, the applied waveform potential diagram during the cyclic voltammetric measurements is shown. The potential waveform consists of three parts; (a) Potential steps, $E_{c1}$ and $E_{c2}$ (which are used for the oxidation and reduction of the electrode surface, respectively), during which the electrochemical cleaning of the electrode surface takes place, (b) $E_c$, where the analyte accumulation happens, and (c) the potential ramp, where the current measurements occur.

During the scan, some of the adsorbed analyte molecules are desorbed. Depending on the rate of those processes and scan rate, the amount of desorption analyte molecules can be changed. The important point here is that: part of the adsorbed analyte molecules still remain on the electrode surface, inhibiting the red/ox process of the electrode surface. In this technique, $\Delta Q$ is calculated in accordance with all current changes at the CVs [42–46].

One of the considerable aspects of this method is application of a special digital filtration, which is applied during the measurement. At first, an electrode CV was recorded and then by applying FFT on the collected data, the existing high frequency noises were indicated. With the aid of this information, the cutoff frequency of the analog filter was set at a certain value (where the noises were removed from the CV).

Since the crystal structure of a polycrystalline gold electrode is greatly affected by the condition of the applied potential waveform [37], different potential waveforms were examined to obtain a reproducible electrode surface (or a stable background signal). In fact, the application of cyclic voltammetry for the determination of electroactive compounds mainly faces low stability of the background signal. This is due to the changes taking place in the surface crystal structure during the oxidation and reduction of the electrode in each potential cycle.

The electrochemical oxidation process of the gold surface starts with the hydroxyl ion electrosorption, which at more positive potentials results in the gold oxide formation undergoing structural rearrangement [47].

An example of the recorded CVs is demonstrated in Fig. 3a and b. Figure 3a shows a CV sequence recorded during the flow analysis for lanthanide determination. The injection volume was 50 μL of (1.0 mg $L^{-1}$) $Ho^{3+}$, $Er^{3+}$, $Tm^{3+}$, $Yb^{3+}$, and $Lu^{3+}$ (in 0.05 M $H_3PO_4$) into the eluent

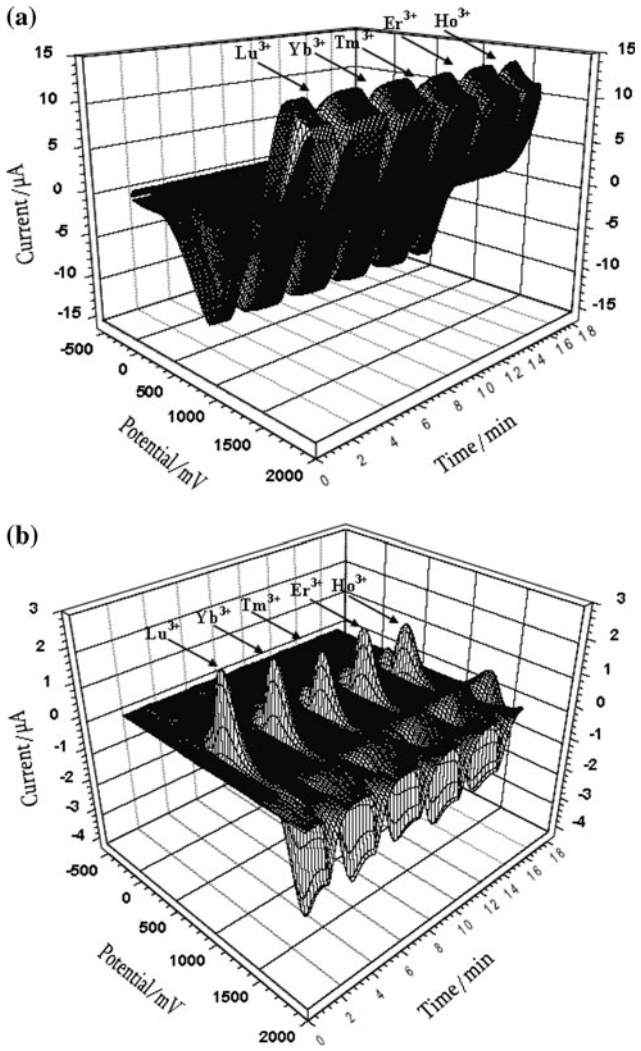


**Fig. 3** **a** Cyclic voltammogram at 12.5 μm Au ultramicroelectrode recorded during a flow injection experiment. The eluent was 0.05 mol $L^{-1}$ $H_3PO_4$, the flow rate was 100 μL $s^{-1}$, and the sweep rate was 30 V $s^{-1}$. Each scan was preceded by 100 ms (at 600 mV) and 100 ms (at −800 mV) conditioning, respectively. The accumulation time was 300 ms at −300 mV. The injected solution (50 μL) contained 1.0 ppm $Ho^{3+}$, $Er^{3+}$, $Tm^{3+}$, $Yb^{3+}$, and $Lu^{3+}$ in 0.05 mol $L^{-1}$ $H_3PO_4$. **b** Curves result from the subtraction of the CVs average (in the absence of the analytes) from the test of the CVs in **a**

solution, containing 0.05 mol $L^{-1}$ $H_3PO_4$. The time axis of the graph represents the time of the flow injection experiment. In the absence of heavy lanthanide ions, the shape of the CV curve is typical for a polycrystalline gold electrode in acidic media [48]. Figure 3b illustrates the absolute current changes in the CVs curves after subtracting the average background of four CVs (in the absence of analytes). Evidently, this way of presenting the electrode response gives more details about the adsorbed ion effect on CV currents. As a matter of fact, the curves show that current changes mainly take place at potential regions of the oxidation and reduction of gold. When the electrode-solution interface is exposed to heavy lanthanide ions, which can be adsorbed on the electrode, the oxide formation process becomes severely inhibited. In detail, the surface process inhibition causes significant change in the currents at the potential region and, as a consequence, the profound changes in the shape of the CVs take place.

Theoretically, the analyte response can be affected by the thermodynamic and kinetic parameters of adsorption, the mass transport rate, and the electrochemical behavior of the adsorbed species. The free energy and the adsorption rate depend on: the electrode potential, the electrode material, and, to some extent, on the choice of concentration and the type of supporting electrolyte. By taking these points into consideration for achievement of the detector maximum performance, the effect of experimental parameters (such as pH of the supporting electrolyte, the potential, accumulation time, and potential scan rate) must be examined and optimized [49–55].

**Table 2** Stability constants (log *K*) of light lanthanides with α-HIBA used as complexing agent at 20 °C

| Lanthanide | log *K* |
|---|---|
| Holmium | 7.96 |
| Erbium | 8.13 |
| Thulium | 8.39 |
| Ytterbium | 8.69 |
| Lutetium | 8.82 |

### 3.2 Experimental parameter optimization

Stability constants of the Ln-eluent complexes affect the elution pattern of lanthanides. If the stability constant of Ln-eluent complex is more, its elution will be faster. The lesser the stability constant of the complex, the slower its elution will be. In general, for all the eluents, the stability constant increases from Ho to Lu and this explains the elution pattern in the order of decreasing atomic number from Lu to Ho in the cation-exchanger. The nature of the metal ion and eluent as well as environmental factors, such as solvent or medium, concentration, temperature and pressure, can affect the formation of a complex between them. Hence, the stability constants for a given metal–eluent complex under different environmental conditions can be different. The log values of stability constant for complexes of light lanthanides with HIBA vary from 7.96 for Ho(III) to 8.82 for Lu(III) as reported in the literature [56] and are given in Table 2. These only give a qualitative picture of the behavior during separation of lanthanides; however, the exact performance can be different.

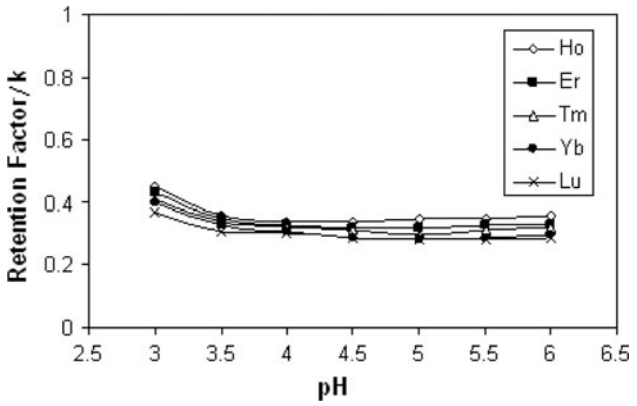


**Fig. 4** Effect of pH of mobile phase on retention of light lanthanides DOWEX 50WX8 under isocratic condition: 0.2 M of HIBA. The injected solution (50 μL) contained 1.0 mg $L^{-1}$ $Ho^{3+}$, $Er^{3+}$, $Tm^{3+}$, $Yb^{3+}$, and $Lu^{3+}$ in 0.05 mol $L^{-1}$ $H_3PO_4$

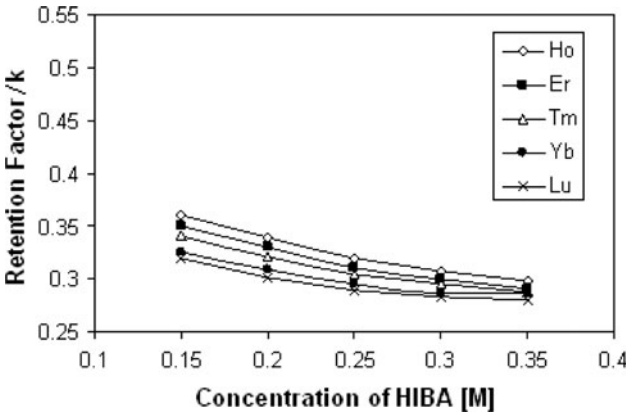


**Fig. 5** Effect of HIBA concentration (pH 4.0) on retention of lanthanides on DOWEX 50WX8. The injected solution (50 μL) contained 1.0 mg $L^{-1}$ $Ho^{3+}$, $Er^{3+}$, $Tm^{3+}$, $Yb^{3+}$, and $Lu^{3+}$ in 0.05 mol $L^{-1}$ $H_3PO_4$

### 3.2.1 *Effect of pH of eluent on retention of lanthanide ions*

Effect of mobile phase pH on the elution pattern of a mixture of light lanthanide ions using HIBA is shown in Fig. 4. This effect was monitored using retention factor ($K$). The analytical expression for $K$ is:

$$K = \frac{(t_R - t_0)}{t_0} \quad (1)$$

In this equation, $t_0$ is retention time of non-retained peak and $t_R$ is retention time of the eluent retained. As it can be seen, increasing pH from 3.0 to 6.0 caused a decrease of retention factor ($K$) for lanthanide ions. Changes in pH have an effect on the elution efficiency of carboxylic acids. This factor depends on its strength, which in turn depends on its pH. The α-hydroxycarboxylic acids tested were all weak acids and undergo only partial ionization, hence, show poor eluting strength at low pH [11]. With increasing pH, the elution efficiency increased due to the greater ionization of the –COOH group. However, at higher pH, the retention factors for different lanthanides are quite close. Therefore, pH = 4.0 was selected as the optimum, which gives adequate resolution in a shorter time. Furthermore, this pH was chosen because it is near to that of the maximum buffer capacity for HIBA.

### 3.2.2 *Effect of concentration of eluent on retention of lanthanide ions*

The influence of the concentration of HIBA on retention of heavy lanthanides is shown in Fig. 5. In high concentrations of eluent, elution of lanthanides is faster. The effect of concentration of HIBA was studied at pH 4.0. Under this condition, HIBA is ~63% ionized ($pK_a = 3.77$) [57]. With an increase in concentration of α-HIBA, the concentration of α-hydroxyisobutyrate ions increases in the mobile phase and these results in faster elution of lanthanides on the column.

### 3.2.3 *Influence of sweep rate, accumulation potential, and accumulation time*

For the investigation of the scan rate's influence and the eluent flow rate on the sensitivity of the detector response, solutions having a concentration of 1.0 ppm of $Ho^{3+}$, $Er^{3+}$, $Tm^{3+}$, $Yb^{3+}$, and $Lu^{3+}$ were injected. At different scan rates (from 5 to 100 V $s^{-1}$) and eluent flow, the detector responses of the injected sample were recorded. These results are presented in Fig. 6. As it is clear from Fig. 6a, the detector exhibits the maximum sensitivity at the scan rate of 30 V $s^{-1}$, and Fig. 6b shows that flow rate of 3 mL $min^{-1}$ is the best. The effects of sweep rate on detection performance can be considered in three different aspects: first, speed in data acquisition; second, kinetic factors of lanthanide ions adsorption, and, finally, the eluent flow rate which controls the time window of the solution zone in the detector. The main reason for the application of high scan rates is prevention from desorption of the adsorbed lanthanide ions during the potential scanning (because under this condition, the inhibition outcome of the adsorbed lanthanide ions on the oxidation process can take place).

It is a fact that employment of high scan rates is required for use of this detection method in conjunction with fast separation techniques, such as capillary electrophoresis. From this point of view, it is necessary to check how the method sensitivity is affected by the sweep rate. Therefore, high sweep rates must be employed to detect the amount of the adsorbed analyte on the electrode surface, so that the potential scanning step is short in comparison with the accumulation period. An important point to be taken into

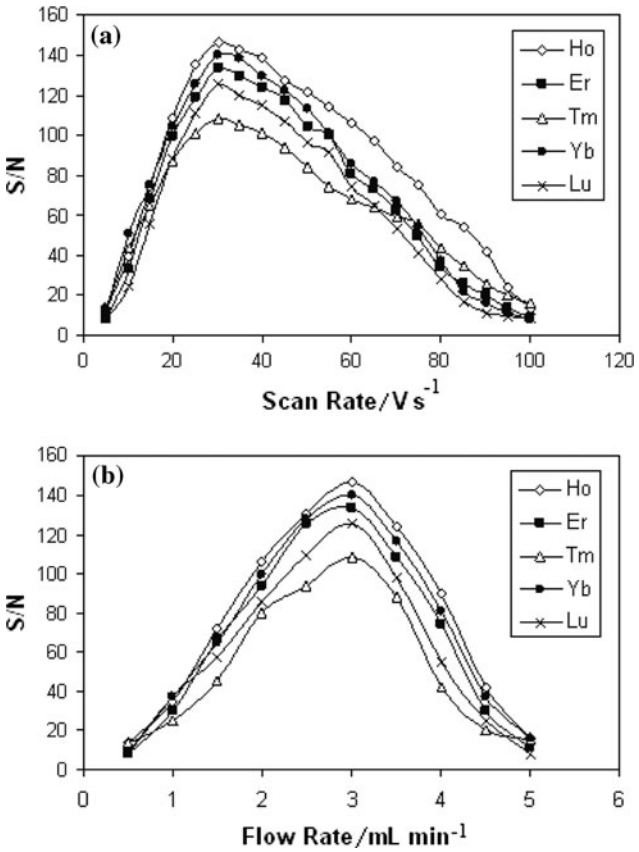


**Fig. 6** **a** The effect of the sweep rate and **b** the effect of flow rate on the response of the Au electrode (with a radius of 12.5 μm) to injections of 1.0 mg $L^{-1}$ $Ho^{3+}$, $Er^{3+}$, $Tm^{3+}$, $Yb^{3+}$, and $Lu^{3+}$ in 0.05 mol $L^{-1}$ $H_3PO_4$

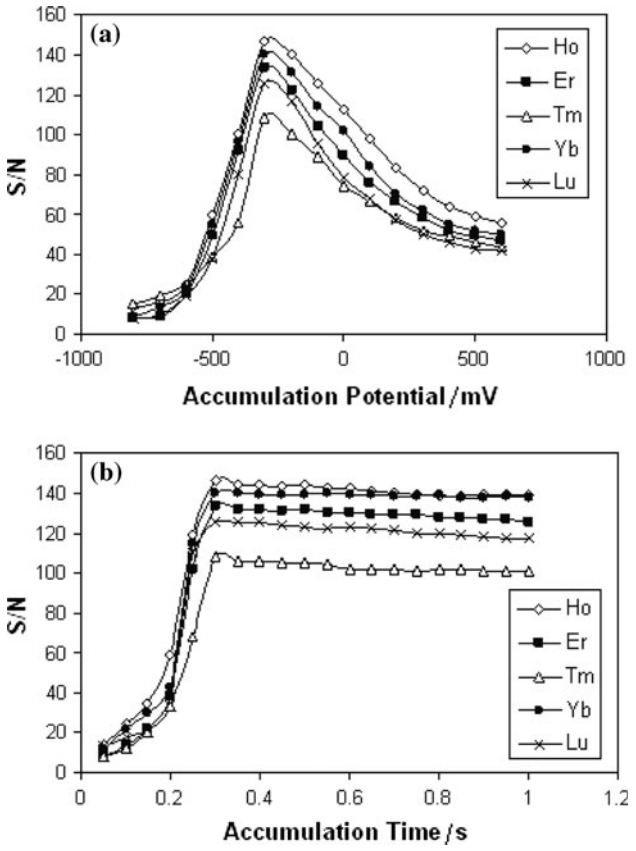


**Fig. 7** **a** The effect of accumulation potential and **b** the effect of accumulation time on electrode response to injections of 1.0 mg $L^{-1}$ $Ho^{3+}$, $Er^{3+}$, $Tm^{3+}$, $Yb^{3+}$, and $Lu^{3+}$ in 0.05 mol $L^{-1}$ $H_3PO_4$

consideration is the time when the accumulation of lanthanide ions occurs at a potential that is greater or smaller than $E_i$. However, the sensitivity of the detection system mainly depends on the potential sweep rate, mostly due to the adsorption kinetic factors and the instrumental limitations. Notably, any changes in parameters relating to the adsorption process and affecting the applied potential (time and potential of accumulation), severely influences the sensitivity of the measurement. For this reason, the influence of the accumulation potential and response time of the method for injection of 1.0 mg $L^{-1}$ solution of $Ho^{3+}$, $Er^{3+}$, $Tm^{3+}$, $Yb^{3+}$, and $Lu^{3+}$ in 0.05 mol $L^{-1}$ $H_3PO_4$, was studied. Figure 7 shows the detector response over the accumulation potential ranges of −800 to 600 mV, and the accumulation time range of 0.05–1.0 s. Figure 7a and b derives the conclusion that optimum conditions to be chosen are: accumulation potential of −300 mV and accumulation time of 300 ms, on the grounds that the electrode surface becomes saturated with lanthanide ions within a 1,300 ms time window.

On the electrode, lanthanide ions accumulation takes place during the accumulation step (assuming that an appropriate potential is selected). The difference in the saturation time of various compounds can be related to existing differences in their kinetics of electron transfer and mass transport. As mentioned above, the surface of the gold ultra microelectrode is small and, in a short time, the surface can be saturated.

### 3.3 Validation

The method was validated in terms of linearity, limit of quantitation (LOQ), limit of detection (LOD), precision, accuracy, ruggedness/robustness, recovery, and selectivity.

The linearity was evaluated by linear regression analysis, which was calculated by the least square regression method. The calibration curves obtained for heavy lanthanide ions were linear over the concentration range of 140–18,000 μg $L^{-1}$. The peak areas of $Ho^{3+}$, $Er^{3+}$, $Tm^{3+}$, $Yb^{3+}$, and $Lu^{3+}$ were plotted versus its concentration and linear regression analysis was carried out on the resultant curve. After this analysis, a correlation coefficient of $R = 0.999$ and %RSD values, ranging from 0.28 to 3% across the studied concentration range, were obtained. Typically, the regression equation for the calibration curve

was found to be $Y = 0.0025X + 120.12$, $Y = 0.0027X + 26.939$, $Y = 0.0029X + 77.502$, $Y = 0.0015X + 27.903$, and $Y = 0.0017X + 19.598$ for $Ho^{3+}$, $Er^{3+}$, $Tm^{3+}$, $Yb^{3+}$, and $Lu^{3+}$, respectively. Figure 8 depicts the calibration graph that resulted from the monitoring of these lanthanide ions in a 0.05 mol $L^{-1}$ $H_3PO_4$.

Concerning the LOD value, it was measured as the lowest analyte amount that may be detected to produce a response, which is significantly different from that of a blank one. The limit of detection was approved by calculations based on the standard deviation of the response ($\delta$) and the slope ($S$) of the calibration curve, at the levels approaching the limits according to the equation LOD = 3.3 ($\delta/S$) [58]. The LOD for $Ho^{3+}$, $Er^{3+}$, $Tm^{3+}$, $Yb^{3+}$, and $Lu^{3+}$ was found to be 50 μg $L^{-1}$. On the other hand, the LOQ was measured as the lowest analyte amount that can be reproducibly quantified above the baseline noise, for which triplicate injections resulted in an RSD $\leq$ 1.19%. A practical LOQ, giving a good precision and acceptable accuracy, was equivalent to 140 μg $L^{-1}$.

The precision of the assay was investigated with respect to both repeatability and reproducibility. The repeatability was investigated by injecting nine replicate samples each of 140, 8,000, and 18,000 μg $L^{-1}$ standards. In addition, injecting the same three concentrations over three consecutive days assessed inter-day precision. The results are in Table 3.

Regarding the accuracy of the assay, it was determined by the interpolation of replicate ($n = 6$) peak areas of three accuracy standards 140, 8,000, and 18,000 μg $L^{-1}$ from a

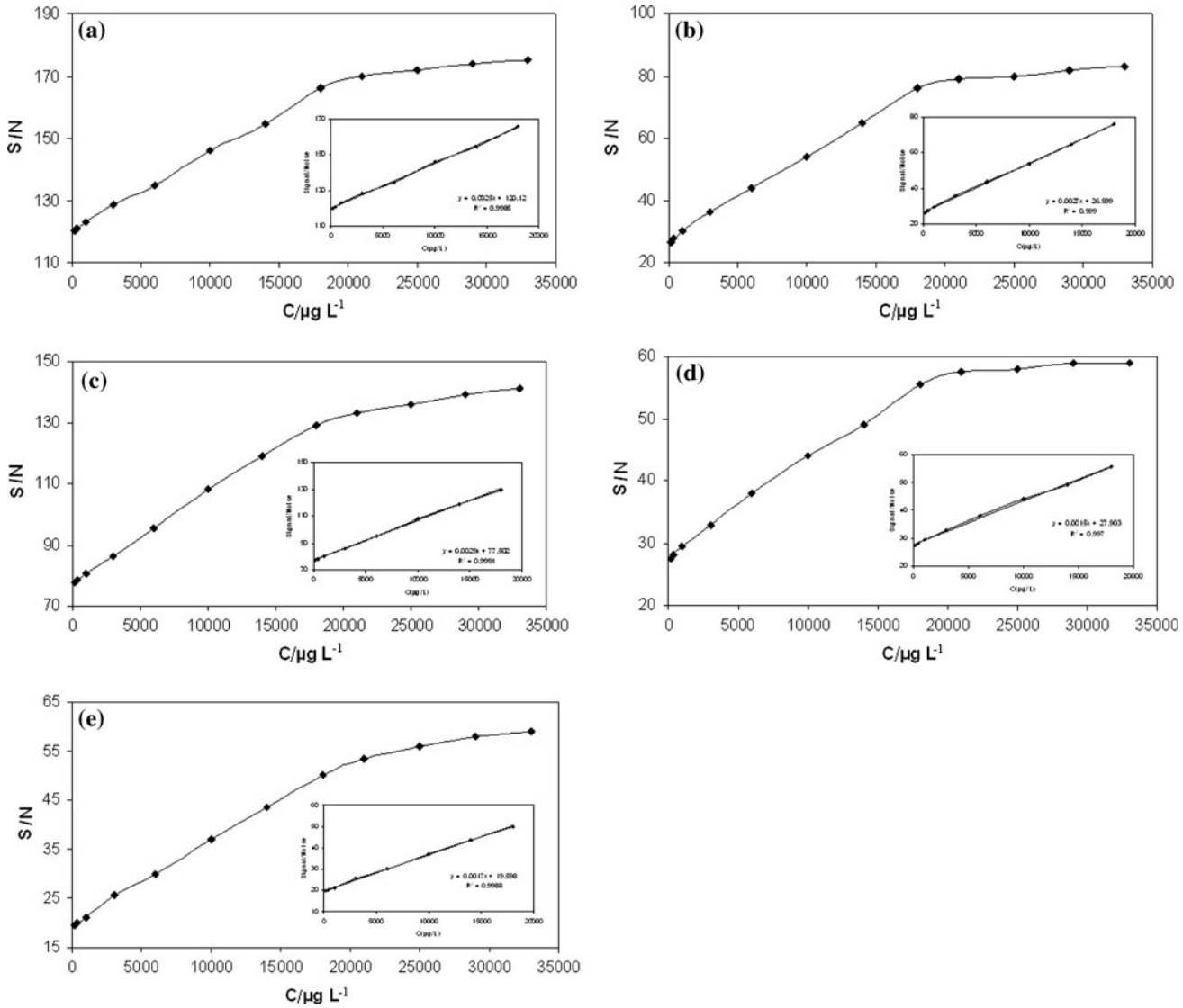


**Fig. 8** Calibration curves obtained for **a** $Ho^{3+}$, **b** $Er^{3+}$, **c** $Tm^{3+}$, **d** $Yb^{3+}$, and **e** $Lu^{3+}$ ions on the Au electrode in 0.05 M $H_3PO_4$ under isocratic condition: 0.2 M of HIBA, Scan rate: 30 V $s^{-1}$, Flow rate: 3 mL $min^{-1}$

**Table 3** Precision and inter-day precision of the assay

| | Standard solutions ($\mu g\ L^{-1}$) | Precision | | Inter-day precision | |
|---|---|---|---|---|---|
| | | Mean concentration ($\mu g\ L^{-1}$) | RSD (%) | Mean concentration ($\mu g\ L^{-1}$) | RSD (%) |
| $Ho^{3+}$ | 140 | 145 | 2.44 | 152 | 2.89 |
| | 8,000 | 8,012 | 1.86 | 8,017 | 2.52 |
| | 18,000 | 17,923 | 0.87 | 17,911 | 1.53 |
| $Er^{3+}$ | 140 | 147 | 2.83 | 153 | 3.05 |
| | 8,000 | 8,017 | 2.26 | 8,023 | 2.31 |
| | 18,000 | 17,947 | 0.88 | 17,940 | 1.15 |
| $Tm^{3+}$ | 140 | 143 | 2.65 | 145 | 3.05 |
| | 8,000 | 8,020 | 2.13 | 8,033 | 2.64 |
| | 18,000 | 17,909 | 1.00 | 17,900 | 1.53 |
| $Yb^{3+}$ | 140 | 148 | 3.07 | 151 | 2.52 |
| | 8,000 | 8,009 | 1.58 | 8,014 | 2.00 |
| | 18,000 | 17,953 | 1.00 | 17,941 | 1.15 |
| $Lu^{3+}$ | 140 | 145 | 3.20 | 153 | 3.60 |
| | 8,000 | 8,012 | 2.62 | 8,013 | 2.52 |
| | 18,000 | 17975 | 0.78 | 17,970 | 1.15 |

**Table 4** Accuracy of the assay

| | Standard solutions ($\mu g\ L^{-1}$) | Resultant concentration ($\mu g\ L^{-1}$) | Relevant error (%) |
|---|---|---|---|
| $Ho^{3+}$ | 140 | 144 ± 2 | 2.86 |
| | 8,000 | 8057 ± 35 | 0.71 |
| | 18,000 | 17905 ± 41 | 0.53 |
| $Er^{3+}$ | 140 | 145 ± 1 | 3.57 |
| | 8,000 | 8073 ± 41 | 0.91 |
| | 18,000 | 17922 ± 52 | 0.43 |
| $Tm^{3+}$ | 140 | 143 ± 7 | 2.14 |
| | 8,000 | 8065 ± 26 | 0.81 |
| | 18,000 | 17914 ± 45 | 0.48 |
| $Yb^{3+}$ | 140 | 174 ± 5 | 5.00 |
| | 8,000 | 8122 ± 50 | 1.52 |
| | 18,000 | 17890 ± 15 | 0.61 |
| $Lu^{3+}$ | 140 | 145 ± 2 | 3.57 |
| | 8,000 | 8095 ± 71 | 1.19 |
| | 18,000 | 17900 ± 71 | 0.56 |

calibration curve prepared as previously described. In each case, the relevant error percentage, and the accuracy were calculated. Table 4 shows the resultant concentrations with their relevant error percentage.

The ruggedness of the method was calculated by the comparison of the intra- and inter-day assay results for lanthanide ions undertaken by two analysts. The %RSD values for intra- and inter-day assays of lanthanide ions in the cited formulations, performed in the same laboratory by two analysts, did not exceed 4%; thus, indicating the ruggedness of the method. Also, the robustness of the method was investigated under a variety of conditions such as small changes in pH of eluent, flow rate, buffer composition, and laboratory temperature. As, it can be seen in Table 5, heavy lanthanide ions recovery percentages were good under most conditions, not demonstrating any significant change when the critical parameters were modified.

**Table 5** Influence of the changes in the experimental conditions on the performance of the FIA system

| Parameter | Modification | %Recovery | | | | |
|---|---|---|---|---|---|---|
| | | $Ho^{3+}$ | $Er^{3+}$ | $Tm^{3+}$ | $Yb^{3+}$ | $Lu^{3+}$ |
| pH | 3.9 | 99.7 | 100.3 | 100.9 | 99.4 | 100.4 |
| | 4.0 | 99.9 | 100.4 | 100.9 | 99.9 | 101.2 |
| | 4.1 | 100.0 | 100.0 | 99.1 | 100.1 | 100.8 |
| Flow rate ($mL\ min^{-1}$) | 2.6 | 100.0 | 99.4 | 101.1 | 100.8 | 99.7 |
| | 2.8 | 101.7 | 100.2 | 101.1 | 100.6 | 100.4 |
| | 3.0 | 101.2 | 100.1 | 100.7 | 100.6 | 99.2 |
| Buffer composition ($mol\ L^{-1}$) | 0.20 | 100.4 | 100.2 | 100.2 | 100.7 | 100.6 |
| | 0.19 | 100.8 | 100.3 | 100.6 | 101.9 | 101.2 |
| | 0.18 | 99.2 | 100.4 | 100.5 | 101.4 | 101.0 |
| Lab. temperature (°C) | 20 | 101.4 | 101.3 | 98.2 | 100.9 | 100.7 |
| | 25 | 101.7 | 101.0 | 100.2 | 101.1 | 100.7 |
| | 30 | 101.1 | 99.4 | 100.0 | 100.4 | 100.7 |

Monazite [$(Ln, Th)PO_4$] and Xenotime [$(Y, Ln)PO_4$] are two important lanthanide ores and have large amounts of these elements. The first one is richer in earlier lanthanides and the second one is richer in later lanthanides. Ion-exchange separation is not of real commercial importance for large-scale production, but historically it was a method by which fast high-purity separation of the lanthanides first became feasible [59]. Thus, two solutions were prepared with the same ingredients of monazite and xenotime, and diluted 1,000 times to provide sample solutions (of course, the amounts of holmium, erbium, and ytterbium in xenotime are so large; we diluted them 10 times more than the others). The results obtained for medium lanthanide ions in monazite and xenotime samples under investigation are given in Table 6. For these determinations, five replicate analyses were performed for each sample. The standard deviation of the whole procedure is also given in Table 6. From the results, it can be seen that within the precision of both measuring procedures, the concentration values of these ions determined by FFT-CCV and ICP-AES are in fair agreement.

**Table 6** Comparison between the determination of medium lanthanide ions by FFT-CCV and ICP-AES

| Element | Real amount of monazite solution (mg $L^{-1}$) | Found amount of monazite solution (mg $L^{-1}$) | | Real amount of xenotime solution (mg $L^{-1}$) | Found amount of xenotime solution (mg $L^{-1}$) | |
|---|---|---|---|---|---|---|
| | | FFT-CCV | ICP-AES | | FFT-CCV | ICP-AES |
| Ho | 0.50 | 0.52 ± 0.01 | 0.54 ± 0.04 | 2.00 | 2.08 ± 0.04 | 2.07 ± 0.05 |
| Er | 2.00 | 1.90 ± 0.09 | 1.98 ± 0.21 | 5.40 | 5.55 ± 0.16 | 5.20 ± 0.11 |
| Tm | 0.20 | 0.20 ± 0.03 | 0.22 ± 0.07 | 9.00 | 9.29 ± 0.27 | 9.41 ± 0.38 |
| Yb | 1.00 | 0.87 ± 0.02 | 1.072 ± 0.02 | 6.20 | 6.12 ± 0.22 | 6.04 ± 0.12 |
| Lu | 0.20 | 0.19 ± 0.03 | 0.18 ± 0.05 | 4.00 | 3.94 ± 0.09 | 3.74 ± 0.14 |

**Table 7** Comparison between the detection limits of the proposed method with the other reported methods

| Separation method | Detection method | Detection limit | References |
|---|---|---|---|
| IEC | Vis | ~10 mg $L^{-1}$ | [1] |
| IEC | Vis | 5 mg $L^{-1}$ | [2] |
| HPCIC | Vis | 4 mg $L^{-1}$ | [3] |
| IEC | Spectrofluorimetry | >50 mg $L^{-1}$ | [4] |
| IEC | Spectrofluorimetry | >50 mg $L^{-1}$ | [5] |
| CE | UV | 240–470 mg $L^{-1}$ | [6] |
| SPE-RP-ion pair-HPLC | UV-RI | 10 mg $L^{-1}$ | [7] |
| CE | UV | 530–960 μg $L^{-1}$ | [8] |
| RP-HPLC | UV–Vis | 50 μg $L^{-1}$ | [9] |
| RP-HPLC | Diode array detector | >9 mg $L^{-1}$ | [10] |
| CE | UV | 4.8 mg $L^{-1}$ | [11] |
| IEC | ICP-AES | 50–220 μg $L^{-1}$ | [15] |
| – | Potentiometry | 121 μg $L^{-1}$ | [26] |
| – | Potentiometry | 1.3 mg $L^{-1}$ | [29] |
| – | Potentiometry | 140 μg $L^{-1}$ | [30] |
| – | Potentiometry | 825 μg $L^{-1}$ | [31] |
| – | Potentiometry | 80 μg $L^{-1}$ | [32] |
| – | Potentiometry | 124 μg $L^{-1}$ | [33] |
| – | Potentiometry | 104 μg $L^{-1}$ | [34] |
| – | Potentiometry | 105 μg $L^{-1}$ | [35] |
| IEC | FFT-CCV | 50 μg $L^{-1}$ | This study |

### 3.4 Comparison of the sensitivity of the proposed method and other previous reported methods

Table 7 compares the detection limit of the proposed method with UV–Vis spectrometry, spectrofluorimetry, RI, ICP-AES, and potentiometric methods. As it can be seen, the sensitivity of FFT-CCV method is better than most of them.

## 4 Conclusions

In this study, the cation-exchange separation and determination of holmium, erbium, thulium, ytterbium, and lutetium ions was achieved for the first time by coupling of ion-exchange separation and fast Fourier transform continuous cyclic voltammetry (FFT-CCV) in a flow injection system, thereby enabling direct detection. α-Hydroxyisobutyricacid (HIBA) has been found to be a successful eluent. Lanthanide ions form complexes with HIBA that lowers the affinity of the lanthanide for the cation-exchange resin. Lanthanide ions, such as $Lu^{3+}$ ion, which form a stable complex with HIBA, spend more time in the eluent and elute first. Lanthanide ions, such as $Ho^{3+}$ ion, which form a weaker complex with HIBA, spend relatively less time in eluent and elute later (the rate of transport being in this order $Lu^{3+} > Yb^{3+} > Tm^{3+} > Er^{3+} > Ho^{3+}$). From the results described, it can

be concluded that good separation of these ions can be achieved using isocratic elution with 0.20 mol $L^{-1}$ of HIBA at pH = 4.0. The best values for accumulation potential and accumulation time were −300 mV and 0.3 s, respectively. A 30 V $s^{-1}$ scan rate was necessary. The good agreement between the results obtained by FFT-CCV and ICP-AES indicates that the proposed method has a good accuracy.

## References


1. Knight CH, Cassidy RM, Recoskie BM, Green LW (1984) Anal Chem 56:474
2. Inoue Y, Kumagai H, Shimimura Y (1996) Anal Chem 68:1517
3. Nesterenko PN, Jones PN (1998) J Chromatogr A 804:223
4. Kutun Ş, Akseli A (1999) J Chromatogr A 847:261
5. Kutun Ş, Akseli A (2000) J Chromatogr A 874:311
6. Öztekin N, Erim FB (2000) J Chromatogr A 895:263
7. Buchmeiser MR, Seeber G, Tessadri R (2000) Anal Chem 72:2595
8. Öztekin N, Erim FB (2001) J Chromatogr A 924:541
9. Santoyo E, Verma SP (2003) J Chromatogr A 997:171
10. Raut NM, Jaison PG, Aggarwal SK (2004) J Chromatogr A 1052:131
11. Santoyo E, García R, Galicia-Alanis KA, Verma SP, Aparicio A, Santoyo-Castelazo A (2007) J Chromatogr A 1149:12
12. Henderson P (1984) Rare earth element geochemistry. Elsevier, Amsterdam
13. Barkley DJ, Blanchette M, Cassidy RM, Elchuk S (1986) Anal Chem 58:2222
14. Dufek P, Vobecky M, Holik J, Valasek J (1988) J Chromatogr 435:249
15. Borai EH, Eid MA, Aly HF (2002) Anal Bioanal Chem 372:537
16. Elchuk S, Burns KI, Cassidy RM, Lucy CA (1991) J Chromatogr 558:197
17. Bruzzoniti MC, Mentasti E, Sarzanini C (1997) Anal Chim Acta 353:239
18. Kuroda R, Wada T, Kishimoto G, Oguma K (1991) Chromatographia 32:65
19. Vera-Avila LE, Camacho E (1992) J Liq Chromatogr 15:835
20. Fernández RG, Alonso JIG (2008) J Chromatogr A 1180:59
21. Nuryono C, Huber G, Kleboth K (1998) Chromatographia 48:407
22. Verma SP (1991) Lanthan Actin Res 3:237
23. Kawabata K, Kishi Y, Kawaguchi O, Watanabe Y, Inoue Y (1991) Anal Chem 63:2137
24. Haley BA, Klinkhammer GP (2003) Mar Chem 82:197
25. Tan SH, Horlick G (1986) Appl Spectrosc 40:445
26. Ganjali MR, Norouzi P, Daftari A, Faridbod F, Salavati-Niasari M (2007) Sens Actuat B 120:673
27. Ganjali MR, Pourjavid MR, Rezapour M, Haghgoo S (2003) Sens Actuat B 89:21
28. Ganjali MR, Ravanshad J, Hosseini M, Salavati-Niasari M, Pourjavid MR, Baezzat MR (2004) Electroanalysis 16:1771
29. Ganjali MR, Faridbod F, Norouzi P, Adib M (2006) Sens Actuat B 120:119
30. Ganjali MR, Tamaddon A, Norouzi P, Adib M (2006) Sens Actuat B 120:194
31. Ganjali MR, Rasoolipour S, Rezapour M, Norouzi P, Amirnasr M, Meghdadi S (2006) Sens Actuat B 119:89
32. Zamani HA, Rajabzadeh G, Ganjali MR (2007) Talanta 72:1093
33. Faridbod F, Ganjali MR, Dinarvand R, Norouzi P, Riahi S (2008) Sensors 8:1645
34. Ganjali MR, Memari Z, Faridbod F, Dinarvand R, Norouzi P (2008) Electroanalysis 20:2663
35. Faridbod F, Ganjali MR, Larijani B, Norouzi P, Riahi S, Mirnaghi FS (2007) Sensors 7:3119
36. Kissinger PT, Heineman WR (1984) Laboratory techniques in electroanalytical chemistry. Marcel Dekker, New York
37. Wightman RM, Wipf DO (1989) In: Bard AJ (ed) Electroanalytical chemistry, vol 15. Marcel Dekker, New York
38. Dimitrakopoulos T, Alexander PW, Hibbert DB (1996) Electroanalysis 8:438
39. Cosofret V, Erdosy M, Johnson TA, Buck RP, Ash RB, Neuman MR (1995) Anal Chem 67:1647
40. Baranski AS, Norouzi P, Nelsson L (1996) J Proc Electrochem Soc 96:41
41. Lide DR (1995) CRC handbook of chemistry and physics, 76th edn. CRC Press, Boca Raton, FL
42. Norouzi P, Ganjali MR, Matloobi P (2005) Electrochem Commun 7:33
43. Norouzi P, Nabi Bidhendi GR, Ganjali MR, Sepehri A, Ghorbani M (2005) Microchim Acta 152:123
44. Ganjali MR, Norouzi P, Ghorbani M, Sepehri A (2005) Talanta 66:1225
45. Norouzi P, Ganjali MR, Ghorbani M, Sepehri A (2005) Sens Actuat B 110:239
46. Norouzi P, Ganjali MR, Alizadeh T, Daneshgar P (2006) Electroanalysis 18:947
47. Lipkowski J, Stolberg L (1992) Adsorption of molecules at metal electrodes. VCH, New York
48. Bockris JOM, Conway BE, Yeager E (1980) Comprehensive treatise of electrochemistry. Plenum, New York
49. Norouzi P, Ganjali MR, Shirvani-Arani S, Mohammadi A (2007) J Pharm Sci 96:893
50. Norouzi P, Shirvani-Arani S, Daneshgar P, Ganjali MR (2007) Biosens Bioelectron 22:1068
51. Norouzi P, Daneshgar P, Ganjali MR, Moosavi-Movahedi AA (2007) J Brazil Chem Soc 18:231
52. Norouzi P, Ganjali MR, Daneshgar P (2007) Anal Lett 40:547
53. Norouzi P, Ganjali MR, Hajiaghababaei L (2006) Anal Lett 39:1941
54. Norouzi P, Ganjali MR, Labbafi S, Mohammadi A (2007) Anal Lett 40:747
55. Norouzi P, Ganjali MR, Daneshgar P (2007) J Pharm Toxical Method 55:289
56. Martell AE, Smith RM (1977) Critical stability constants: other organic ligands, vol 3. Plenum, New York, p 28
57. Fuping HP, Haddad PR, Jackson PE, Carnevale J (1993) J Chromatogr 640:187
58. International Conference on Harmonization (ICH) (1996) Topic Q2 B: validation of analytical procedures—methodology. The European Agency for the Evaluation of Medicinal Products, Geneva
59. Cotton S (2006) Lanthanide and actinide chemistry. Wiley, Chichester